Structural Engineering and Mechanics, *Vol. 51, No. 5 (2014) 793-808*
DOI: http://dx.doi.org/10.12989/sem.2014.51.5.793

Topological material distribution evaluation for steel plate reinforcement by using CCARAT optimizer

Dongkyu Lee[1a], Soomi Shin[*2], Hyunjung Park[3b] and Sungsoo Park[4c]

[1]*Department of Architectural Engineering, Sejong University, Seoul, 143-747, Korea*
[2]*Research Institute of Industrial Technology, Pusan National University, Busan, 609-735, Korea*
[3]*Division of Architecture, Silla University, Busan, 617-736, Korea*
[4]*Department of Architectural Engineering, Pusan National University, Busan, 609-735, Korea*

(Received June 2, 2012, Revised May 29, 2014, Accepted June 23, 2014)

Abstract. The goal of this study is to evaluate and design steel plates with optimal material distributions achieved through a specific material topology optimization by using a CCARAT (Computer Aided Research Analysis Tool) as an optimizer, topologically optimally updating node densities as design variables. In typical material topology optimization, optimal topology and layouts are described by distributing element densities (from almost 0 to 1), which are arithmetic means of node densities. The average element densities are employed as material properties of each element in finite element analysis. CCARAT may deal with material topology optimization to address the mean compliance problem of structural mechanical problems. This consists of three computational steps: finite element analysis, sensitivity analysis, and optimality criteria optimizer updating node densities. The present node density based design via CCARAT using node densities as design variables removes jagged optimal layouts and checkerboard patterns, which are disadvantages of classical material topology optimization using element densities as design variables. Numerical applications that topologically optimize reinforcement material distribution of steel plates of a cantilever type are studied to verify the numerical superiority of the present node density based design via CCARAT.

Keywords: node density based design; material topology optimization; CCARAT; node densities; steel plate; reinforcement

1. Introduction

To visually and optimally generate connectivity, i.e., topology, among members and layouts or shapes of structures under both loading and boundary conditions, discrete truss topology optimization methods that use a so-called ground structure approach have been developed to evaluate appropriate reinforced trusses (Hagishita and Ohsaki 2009, Ali *et al.* 2001, Biondini *et al.* 2001). Despite evaluating both optimized topology and shape, the discrete topology optimization method has some shortcomings; in particular, potential solution possibilities determining varied

∗Corresponding author, Senior Researcher, E-mail: shinsumi82@pusan.ac.kr
[a]Assistant Professor, E-mail: dongkyulee@sejong.ac.kr
[b]Associate Professor, E-mail: phj@silla.ac.kr
[c]Professor, E-mail: parks@pusan.ac.kr

http://www.techno-press.org/?journal=sem&subpage=8 ISSN: 1225-4568 (Print), 1598-6217 (Online)

optimal topologies and shapes are substantially blocked due to the use of straight trusses, i.e. one-directional lines as a unit.

To resolve these problems, the so-called continuous topology optimization has been introduced (Andreassen *et al.* 2011, Huang *et al.* 2010, Bendsoe and Kikuchi 1988, Lee *et al*. 2014, Lee *et al*. 2014) as a material approach, i.e., the so-called SIMP (Solid Isotropic Microstructure of Penalization for Intermediate Density). The conventional SIMP determines both optimal topologies and layouts through material density distributions from almost 0 to 1 of specified volume in a domain that maximizes stiffness for a given set of loads and boundary conditions. SIMP can be considered an element-based design of material topology optimization, as it uses element densities as design variables. The density material distribution may evaluate potential possibility of varied optimal shapes and topologies into straight lines.

Element-based design gives rise to problems in topology optimization where material properties are allowed to vary continuously from element to element. This is why final designs of material topology optimization may render as rough layouts, as they are described by raster patterns based on regular grids like finite elements. Increasing the number of finite elements may reduce raster patterns of optimization results, but computational cost may become an issue.

In this study, a specific node-based distribution method of material properties is presented for material topology optimization in linear elastostatic structures. Node densities are considered as optimization design variables. Material properties for finite element analysis are the arithmetic average values of node densities, and are assumed to be uniform within each element. The density, which varies in different regions, is bilinearly interpolated by shape functions on finite elements, and consists of a continuous density function in the design domain. Therefore, the present node density based design leads to smoothing raster layouts and reduces instances of "checkerboard patterns" in comparison to classical element-based design.

CCARAT (Tiyyagura *et al.* 2007, CARAT 2000) is Computer Aided Research Analysis Tool, which is developed and maintained at the Institute of Structural Mechanics of University of Stuttgart in Germany. The research code CCARAT is a multipurpose finite element program covering a wide range of applications in computational mechanics, including multi-field and multi-scale problems, structural and fluid dynamics, material modeling and finite element technology including shape and topology optimization. The code is parallelized using MPI and runs on a variety of platforms. The present node-based topology optimization algorithm belongs to a specific one of the structural topology optimization methods of CCARAT, which uses an optimality criteria method (Chan *et al*. 2008, Chan 2005), extended to update densities by using type A of Sigmund (2001) and type B of Maute (1995).

The type A optimality criteria method updates element densities, which are then assigned to node densities, i.e., input data for bilinear interpolation of shape function. This procedure makes element densities re-distribute into node densities. The type B optimality criteria method directly updates node densities, which are input data for bilinear interpolation of shape function. This procedure makes node densities re-distribute into element densities.

Numerical applications topologically optimizing reinforced material distribution of steel plates of a cantilever are studied to verify numerical superiority and practical use of the present node density based design via CCARAT.

The remainder of this study is as follows. With respect to SIMP formulation, static material topology optimization problems based on node densities as design variables including node density sensitivity are outlined in Section 2. Section 3 describes checkerboard mode control strategies in node density based material distributions. Section 4 presents type A and B including

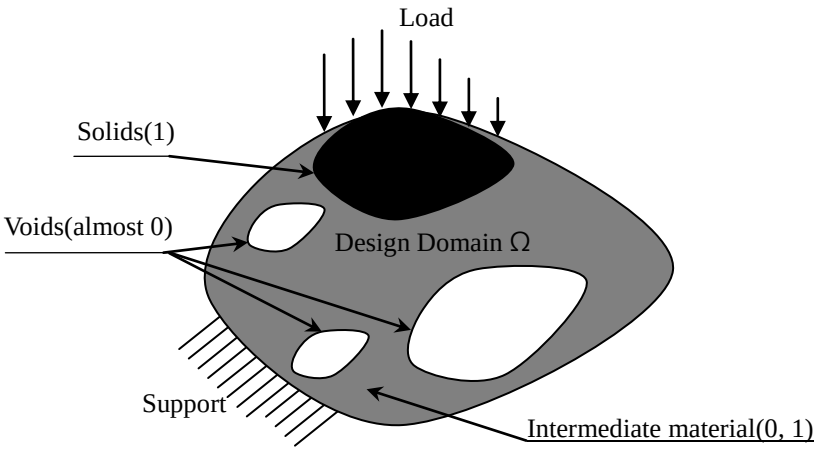

Fig. 1 Design domain for two phase material topology optimization problems of structure

numerical procedures for node-based material topology optimization into a CCARAT optimizer algorithm. The appropriate optimal layouts of deep beams like a cantilever type conformed to load currency, and the optimal shape and topology extraction are studied in several numerical applications of the present method in Section 5. Section 6 presents some conclusions of this study.

2. Node density based topology optimization problems

Conventionally the field of continuous material topology optimization deals with material distributions of voids (density=almost 0, white)-solids (density=1, black)-intermediate states (almost 0<density<1, gray) in a given design space. The schematic of the topology optimization with two material phases under the specified field and boundary conditions for the linear elastostatic problem is shown in Fig. 1.

2.1 Optimization formulations for the linear elastostatic problem

The general problem of structural topology optimization is specified as objective function and constraints. Please note that according to the principle of minimum potential energy objective function can be written as minimum compliance, i.e., minimal strain energy for static problems as follows

$$f = \frac{1}{2}\int_{\Omega_x} \delta\boldsymbol{\varepsilon}^T \mathbf{C}\boldsymbol{\varepsilon}\ d\Omega_x \tag{1}$$

where f and $\boldsymbol{\varepsilon}$ are objective function and strain, respectively. $\mathbf{C}$ is continuous material tensor, which depends on the density-stiffness relationship of SIMP approach (please see Eqs. (4) and (6)) in discretizing a given design space.

The minimal compliance problem aims to design the stiffest or least compliant structure using a given fixed load, the possible support conditions, and the restrictions on the volume of material

used.

The inequality optimization constraint is $0<\Phi\leq 1$, which ensures that density stays within reasonable bounds. Equality constraints are linear elastostatic equilibrium, which clearly presents the state equation, and an equation controlling the volume of the material used under the volume fraction V_{ref} as follows, respectively.

$$\int_{\Omega_x} \delta\boldsymbol{\varepsilon}^T \mathbf{C}\boldsymbol{\varepsilon}\, d\Omega_x = \int_{\Omega_x} \delta\mathbf{u}^T \bar{\mathbf{b}}\, d\Omega_x + \int_{\Gamma_t} \delta\mathbf{u}^T \bar{\mathbf{t}}\, d\Gamma_t \tag{2}$$

$$\int_{\Omega_x} d\Omega_x - V_{ref} = 0 \tag{3}$$

2.2 Interpolation scheme by using SIMP material

After discretization of the continuous design domain, the material density Φ_i^h arithmetically averaged by node densities is constantly assigned to each finite element and is defined by applying a penalty contour to the design variable field, i.e., as in the so-called "power law" or "SIMP approach" (Andreassen *et al.* 2011, Bendsoe *et al.* 1988). According to the SIMP approach, the material density distribution affects element stiffness, and the element stiffness-density relationship may be expressed in terms related to Young's modulus E_i^h, and is associated with the updated element density Φ_i^h arithmetically averaged by node densities and is defined as

$$E_i^h\left(\Phi_i^h\right) = E_0\left(\frac{\Phi_i^h}{\Phi_0}\right)^k, \quad k \geq 1,\ 0 \leq \Phi_i^h \leq 1,\ i = 1\cdots N_e \tag{4}$$

where E_0 and Φ_0 denote the nominal values of Young's modulus and material density of element arithmetically averaged by node densities, respectively, and N_e is the number of elements.

According to the penalized Young's module, element stiffness matrix of four-node square elements with eight-DOF used in this study is written as

$$\boldsymbol{K}_e = \int_V \boldsymbol{B}^T \mathbf{C} \boldsymbol{B}\, dV = \frac{E_i^h\left(\Phi_i^h\right)}{1-\nu^2} \begin{bmatrix} k_1 & k_2 & k_3 & k_4 & k_5 & k_6 & k_7 & k_8 \\ \cdot & k_1 & k_8 & k_7 & k_6 & k_5 & k_4 & k_3 \\ \cdot & \cdot & k_1 & k_6 & k_5 & k_4 & k_3 & k_2 \\ \cdot & \cdot & \cdot & k_1 & k_8 & k_3 & k_2 & k_5 \\ \cdot & \cdot & \cdot & \cdot & k_1 & k_2 & k_3 & k_4 \\ \cdot & \cdot & \cdot & \cdot & \cdot & k_1 & k_8 & k_7 \\ \cdot & \cdot & \cdot & \cdot & \cdot & \cdot & k_1 & k_6 \\ sym. & \cdot & \cdot & \cdot & \cdot & \cdot & \cdot & k_1 \end{bmatrix} \tag{5}$$

where $k_1 = \frac{1}{2} - \frac{\nu}{12}$, $k_2 = \frac{1}{8} + \frac{\nu}{8}$, $k_3 = -\frac{1}{4} - \frac{\nu}{12}$, $k_4 = -\frac{1}{8} + \frac{3\nu}{8}$, $k_5 = -\frac{1}{4} + \frac{\nu}{12}$, $k_6 = -\frac{1}{8} - \frac{\nu}{8}$, $k_7 = \frac{\nu}{6}$, $k_8 = \frac{1}{8} - \frac{3\nu}{8}$

Please note that the stiffness formulation is used for both static and dynamic problems in this study. For example, an isotropic material model with a plane stress (such as a wall structure) is used here without loss of generality, so that

$$\mathbf{C}_i^h = \frac{E_i^h\left(\Phi_i^h\right)}{1-\nu^2}\begin{bmatrix} 1 & \nu & 0 \\ \nu & 1 & 0 \\ 0 & 0 & \frac{1-\nu}{2} \end{bmatrix} \tag{6}$$

where $\mathbf{C}_i^h$ is a material tensor of each finite element *i* and includes the updated term of Young's modulus E_i^h which has been defined by the updated element density average Φ_i^h. *v* is Poisson's ratio.

2.3 Sensitivity analyses

In general, the sensitivity of the optimization problems such as objective functions or constraints is mainly calculated using analytical methods due to small error. The analytical variational approach is used here, as it is numerically more efficient than the discrete method for certain optimization problems. With respect to design variables s (for example, material node densities), the total differential form (Gerzen and Barthold 2012, Amstutz 2011, Haug *et al.* 1986) of the objective function is the combination of parts of an explicit partial derivative and an implicit partial derivative as follows.

$$\nabla_s f \;=\; \nabla_s^{ex} f \;+\; \overline{\nabla}_u f^T \nabla_s \mathbf{u} \tag{7}$$

According to the static topology optimization problem, under the assumptions that external forces $\bar{\mathbf{b}}$, $\bar{\mathbf{t}}$, the differential matrix **L** and a Jacobi matrix **J** are independent of the design variables, the total partial derivative is written as a simple continuous formulation as

$$\nabla_s f = \frac{1}{2}\int_{\Omega_x} \boldsymbol{\varepsilon}^T \nabla_s \mathbf{C}(\Phi)\boldsymbol{\varepsilon}\, d\Omega_x \tag{8}$$

3. Node density based material distribution

3.1 Checkerboard mode control strategy

The origin of checkerboard patterns when using element based design is unclear, but it will be shown in this Section that it is purely a numerical phenomenon, not a physical one. The checkerboard patterns may be reduced by some methods. In this study, node-based design is

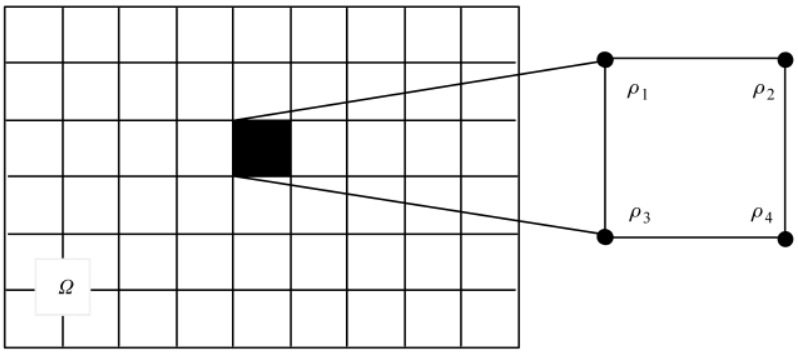

(a) Patch PI by four nodes

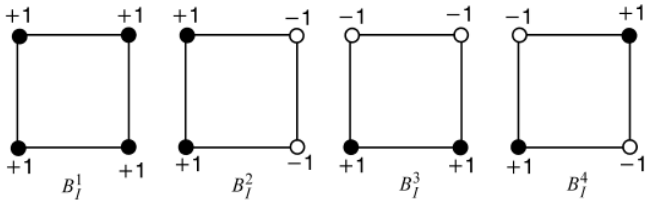

(b) Basis function related with patch

Fig. 2 Patch and basis function for checkerboard mode control

presented in the fields of material topology optimization. It uses node densities as design variables.

Consider a patch P_I of four connective nodes, ρ_1, ρ_2, ρ_3, and ρ_4 as shown in Fig. 2. By association with P_I, the so-called basis function B_I^1, B_I^2, B_I^3, and B_I^4 (Ma *et al.* 2011, Byun *et al.* 2004) take the values by patterns as shown in Fig. 2. They are zero outside P_I. The basis functions $B_I^\kappa(\kappa=1,2,3,4)$ are an orthogonal basis for a given design domain. A pure checkerboard pattern is written as

$$d = \sum_{P_I} d_I B_I^4 \tag{9}$$

where d is the pattern of densities in the entire design domain and d_I is the density pattern in the patch P_I. This suggests that in order to avoid the formulation of checkerboard patterns, we need to restrict density distribution to lie within the more restricted, checkerboard-free space. Following a simple scheme is one way to implement such restrictions. For each patch P_I in a given design domain, let ρ_1, ρ_2, ρ_3, and ρ_4 be node densities at the four nodes of the patch.

The density in the patch can be written as

$$\rho(x) = c_1 B^1 + c_2 B^2 + c_3 B^3 + c_4 B^4 \tag{10}$$

where c_i is a known constant that depends on $\rho_i(i=1,2,3,4)$. x denotes the position of densities in the patch. Within the patch, we need to seek a new density distribution $\bar{\rho}$, and it is described as

$$\bar{\rho}(x) = \bar{c}_1 B^1 + \bar{c}_2 B^2 + \bar{c}_3 B^3 + \bar{c}_4 B^4 \tag{11}$$

where $\bar{\rho}$ is free of checkerboard patterns, i.e., $\bar{c}_4 = 0$ and preserves the amount of material

within the patch such as

$$\int_{P_I} \overline{\rho}\ \mathrm{d}\Omega = \int_{P_I} \rho\ \mathrm{d}\Omega \tag{12}$$

The best approximation to ρ in P_I can be written as

$$\begin{Bmatrix} \overline{\rho}_1 \\ \overline{\rho}_2 \\ \overline{\rho}_3 \\ \overline{\rho}_4 \end{Bmatrix} = \begin{bmatrix} 3/4 & 1/4 & 1/4 & -1/4 \\ 1/4 & 3/4 & -1/4 & 1/4 \\ 1/4 & -1/4 & 3/4 & 1/4 \\ -1/4 & 1/4 & 1/4 & 3/4 \end{bmatrix} \begin{Bmatrix} \rho_1 \\ \rho_1 \\ \rho_1 \\ \rho_1 \end{Bmatrix} \tag{13}$$

The new node densities are then interpolated as element densities by using first order shape function. Therefore, final density distribution of element level in the patch is described as

$$\Phi_I = \frac{\sum_i \overline{\rho}_i}{4} = \frac{\sum_i \rho_i}{4} \tag{14}$$

where Φ_I is new distributions of element densities, which are arithmetic means of node densities. When element densities are calculated from node densities, the results are equal to those of node-based design without using the method (Ma *et al.* 2011, Byun *et al.* 2004), which utilizes the interpolation by first order shape functions about four nodes.

3.2 Numerical strategy transferring between element and node densities

An exchange process between element and node densities is described in Fig. 3. In type A using Sigmund's OC algorithm (Andreassen *et al.* 2011, Sigmund 2001), the element-to-node process is executed to resolve sensitivities of node level, i.e., with respect to node densities. In addition, a node-to-element process is carried out to produce average densities of element level, i.e., element densities. In type B using Maute's OC algorithm (Maute and Ramm 1995), element-to-node and node-to-element processes are sequentially carried out to take average densities of element level. The process that transfers element level into node level, i.e., the element to node process, may be resolved by the process in Fig. 3. The process can be described simply as

$$\rho = \frac{\sum^i \Phi_I A_I}{\sum^J A} \tag{15}$$

where Φ_I denotes the property of element level such as element densities or element sensitivities and ρ is the property of node level such as node density or node sensitivity. A_I is an element area contacted to applied node in 2 dimensional area. A is an area of each element. i is the number of categories of applied node, for example, 1 for edge nodes, 2 for boundary nodes, and 4 for internal nodes. I is an element number contacted to applied node and J is the total number of elements. When it is assumed that areas of all elements take the same values, Eq. (15) is finally rewritten in a simple form as follows

$$\Phi = \frac{\sum^4 \rho_k}{4} \tag{16}$$

where *k* is 1, 2, 3 and 4 in four nodes.

4. OC optimizer of CCARAT for material topology optimization

Algorithmic types of node-based design as shown in Fig. 3 are applied to CCARAT program. Type A uses OC, i.e., optimality criteria, algorithm of node level as an optimization strategy (Andreassen *et al.* 2011, Sigmund 2001). OC algorithm takes node level in type A. Due to the duality between sensitivity analyses of node-based design and element-based design, the algorithm in type A carries out sensitivity analysis at the element level, which has less cost than an analysis at the node level. After sensitivity analysis, sensitivity results at the element level are transformed into those of node level to solve OC method. For square square finite element with four nodes, sensitivity solutions of objective with respect to element densities are divided as a value 4, and the divided values are assigned on each node region. Then, the divided values are added and assigned on each node region according to node categories, with 1 assigned for edge nodes, 2 for boundary nodes, and 4 for internal nodes. Each node includes sensitivity of node level. Finally the node sensitivity values take compensated values by categories of each node, for example, 4 for edge

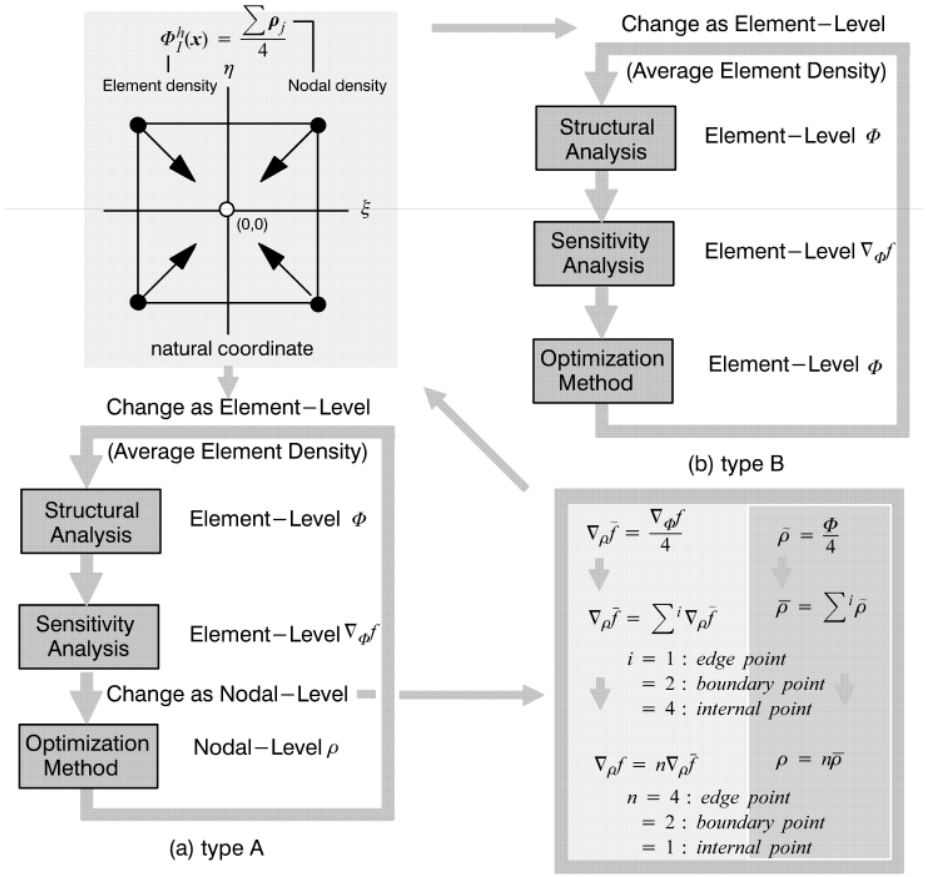

Fig. 3 Systematic CCARAT algorithm for topology optimization

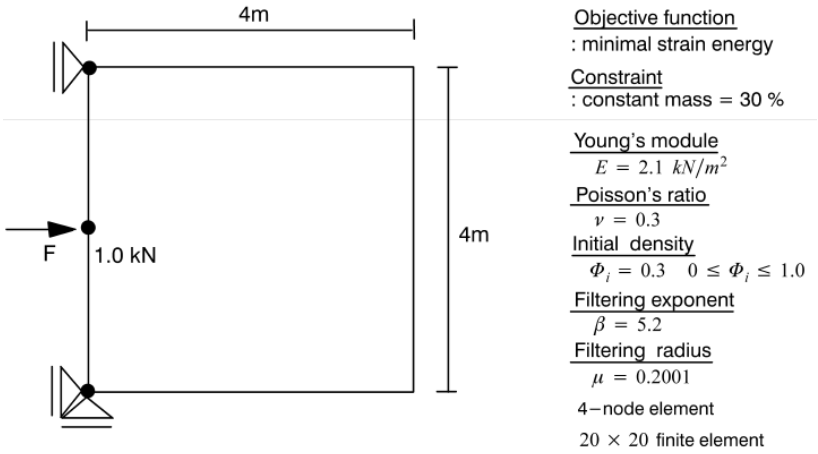

Fig. 4 Definitions of optimization condition for a wall structure such as a deep beam of a cantilever

nodes, 2 for boundary nodes, and 1 for internal nodes. Since finite element analysis is calculated by element level of element stiffness matrix, node densities updated by the OC method are exchanged by updated average element densities in type A, utilizing a bilinear interpolation method, which is also applied to type B.

Type B uses the OC method of element level (Maute and Ramm 1995). In type B all optimization procedures such as finite element analysis, sensitivity, and optimization methods, are performed at the element level. Exchange between element and node densities and average element densities are only needed in CCARAT.

Fig. 3 sketches a typical topology optimization procedure consisting of structural analyses, sensitivity analyses, and optimization methods. Please note that from the solution of the shape and topology design proper truss models for strut-and-tie model design can be automatically produced. This is a key point in this study.

The developed MATLAB code for dynamic topology optimization design is based on MATLAB code (Andreassen *et al.* 2011, Sigmund 2001) for static designs.

5. Numerical applications and discussion

As test examples for practical use, a wall structure like a steel plate of a cantilever type is considered to verify the appropriateness of the present node based design for continuous material topology optimization. The 4 m×4 m wall structure is discretized to be a mesh with 20×20 finite elements, in which an element is a square with four nodes. As material properties considering numerical simplicity, Young's modulus E is assumed to be 2.1 kN/m^2 and Poisson's ratio ν is 0.3. Plane stress is considered. Loading condition P=1.0 kN at the middle point of the left side of the wall structure. Penalty parameter for SIMP material (Andreassen *et al.* 2011, Bendsoe and Kikuchi 1988) is 2.5. For filtering of SIMP, filter exponent β is 2.2 and filter radius μ is 0.35.

The specific volume 30% of total volumes is fixed during every optimization procedure. Objective function is minimal strain energy, i.e., maximal stiffness in the linear elastostatic problem. Optimization problem definitions are shown in Fig. 4.

Table 1 Problem for element and node based topology optimization

Topology Optimization	SIMP	Mesh Independence	Optimization Strategy	Density distribution	Problem Type
Element Based Design (E)	Original (O)	NonFiltering (NF)	OC (O)	Element density	E-O-NF-O
Element Based Design (E)	Original (O)	Filtering (F)	OC (O)	Element density	E-O-F-O
Element Based Design (E)	Regularization (R)	NonFiltering (NF)	OC (O)	Element density	E-R-NF-O
Element Based Design (E)	Regularization (R)	Filtering (F)	OC (O)	Element density	E-R-F-O
Nodal based Design (N)	Original (O)	NonFiltering (NF)	OC of Type A (OA)	Average Element density	N-O-NF-OA
Nodal based Design (N)	Original (O)	Filtering (F)	OC of Type A (OA)	Average Element density	N-O-F-OA
Nodal based Design (N)	Original (O)	NonFiltering (NF)	OC of Type B (OB)	Average Element density	N-O-NF-OB
Nodal based Design (N)	Original (O)	Filtering (F)	OC of Type B (OB)	Average Element density	N-O-F-OB
Nodal based Design (N)	Regularization (R)	NonFiltering (NF)	OC of Type A (OA)	Average Element density	N-R-NF-OA
Nodal based Design (N)	Regularization (R)	Filtering (F)	OC of Type A (OA)	Average Element density	N-R-F-OA
Nodal based Design (N)	Regularization (R)	NonFiltering (NF)	OC of Type B (OB)	Average Element density	N-R-NF-OB
Nodal based Design (N)	Regularization (R)	Filtering (F)	OC of Type B (OB)	Average Element density	N-R-F-OB

Problem types for element and node based topology optimization are illustrated in Table 1. They are classified by variation of element and node based design, variation of SIMP and regularization which is a checkerboard pattern's control in Section 3, variation of original optimality criteria(OC) (Gunwant and Misra 2012, Patnaik *et al.* 1995) and type A of Sigmund or type B of Maute included in CCARAT, and variation of density distribution.

Here, the filter process (Andreassen *et al.* 2011, Sigmund 2001) is a strategy that reduces the checkerboard patterns that may occur in SIMP material in element based design. The present regularization is an alternative to the filter process for node-based design, not element-based design, since regularization is based on the information of node densities within elements (please see the Section 3).

OC algorithm in CCARAT is a heuristic updating scheme for the design parameters (Andreassen *et al.* 2011, Otomori *et al.* 2012). For the heuristic updating scheme used in these numerical examples, updating parameters are defined as follows: *Move*(=1.0E-04) is a positive move limit and *Int*(=1.0) is a maximum interval of design variables. *I_low* (=0.0)is a lower limit of the interval and *I_up* (=1.0)is an upper limit of the interval.

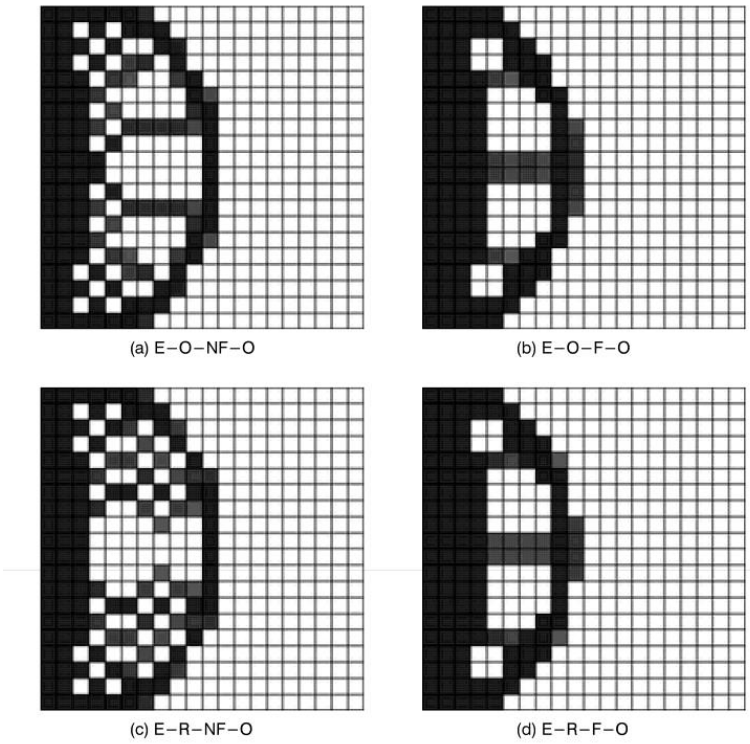

Fig. 5 Optimal results of typical element based design

5.1 Optimal layouts of element based design for material topology optimization

Fig. 5 shows optimal material reinforcement layouts of element-based design which are described by an element density distribution from almost 0 (white) to 1 (black), after optimization iteration of 350.

As can be seen in Fig. 5, element-based design using element densities as design variables leads to jagged boundaries, though a filter method can remove the checkerboard pattern. In Fig. 5(a) and (c), it can be found that there is no regularization effect to remove checkerboard patterns in element-based design.

5.2 Optimal layouts of node based design by using OC of types A and B

Fig. 6 presents optimal material reinforcement layouts of node-based design by using OC of type A which are described by a distribution of element densities arithmetically averaging node densities from almost 0 (white) to 1 (black). The results converged to an optimization iteration of 800. As can be seen in Fig. 6(a), node-based design using node densities as design variables leads to the removal of the checkerboard patterns that occur in element-based design, despite not using the filter method. In addition, node-based design reduces the jagged boundaries between material (solid with 1) and non-material (void with almost 0) in comparisons with the results of element-based design. Since boundaries between solids and voids may be smoothed despite the lack of fine mesh, the computational burden can be reduced until convergence. The optimal layouts including

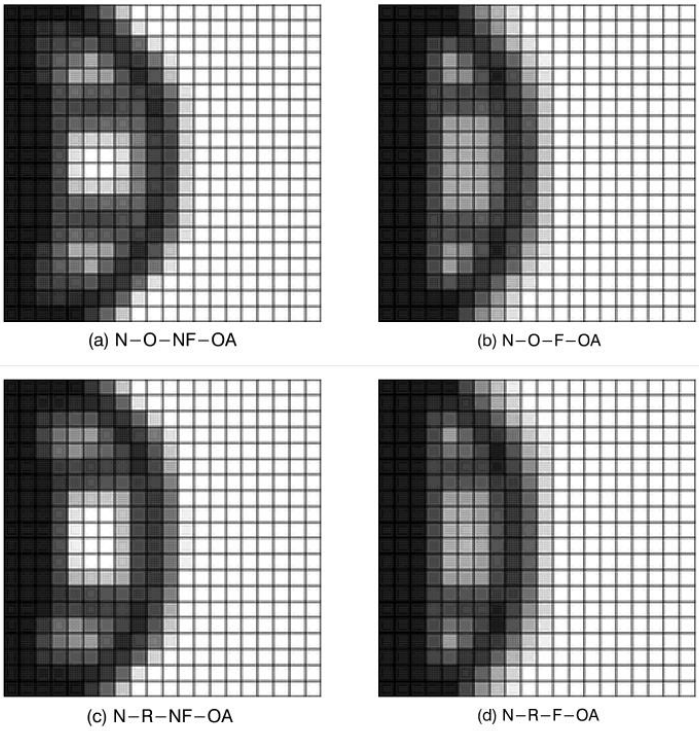

Fig. 6 Optimal results of node based design using OC of type A

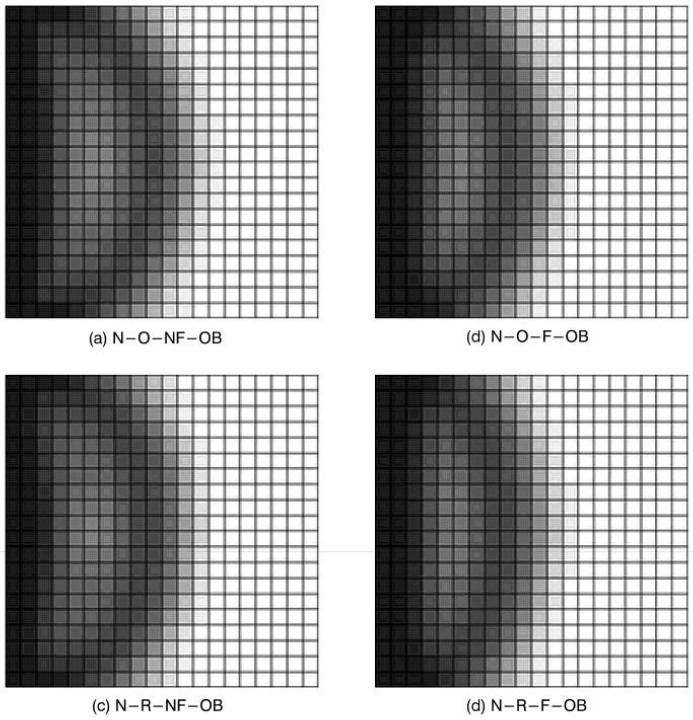

Fig. 7 Optimal results of node based design using OC of type B

intermediate material (gray) may block cracks or collapses at weak regions such as corners. By using the filter method, void regions (white) at the center of the wall structure change to intermediate material regions (gray).

As can be seen in Fig. 6(a) and (c), or in Fig. 6(b) and (d), by using regularization void regions (white) are extended near the center of the wall structure and it seems that locally reducing solid regions prevents the occurrence of checkerboard patterns.

Fig. 7 presents optimal material reinforcement layouts of node-based design by using OC of type B which are described by a distribution of element densities arithmetically averaging node densities from almost 0 (white) to 1 (black). The results converged to an optimization iteration of 800. As can be seen, they are distributed by almost intermediate material regions in which checkerboard patterns and jagged boundaries no longer appear. The use of OC of type B in node based design has a tendency to overcompensate for checkerboard patterns and jagged boundaries.

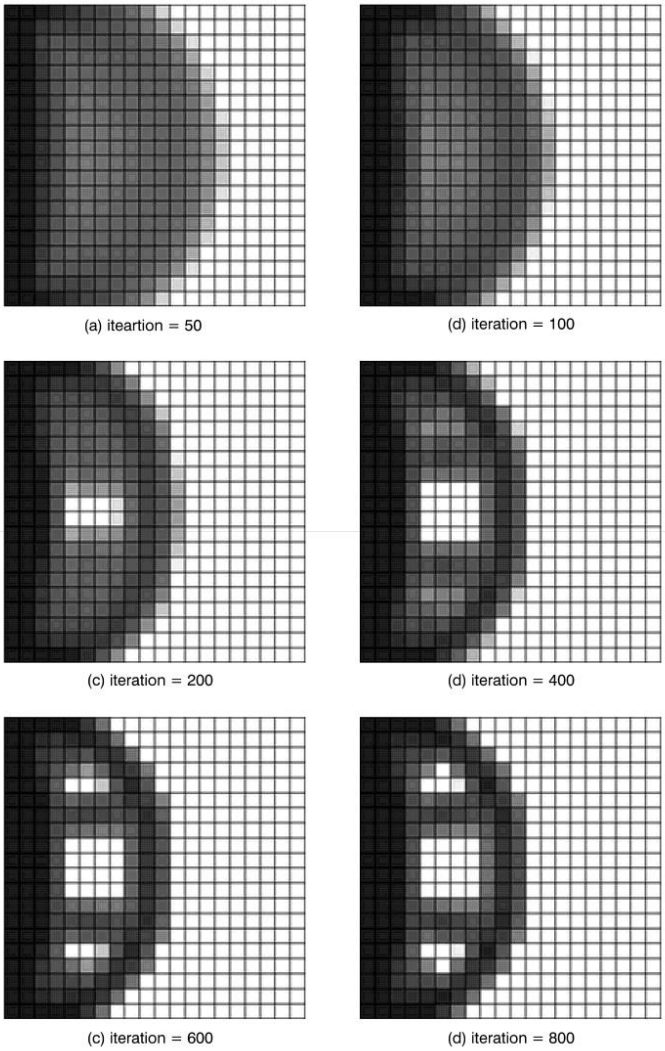

Fig. 8 Convergence histories of node based design of N-O-NF-OA

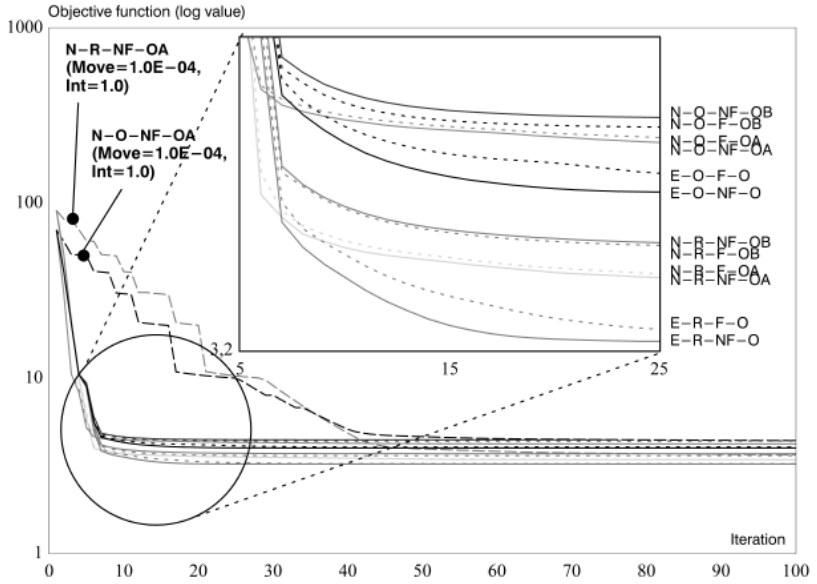

Fig. 9 Convergence curves of objective function in element and node based design

Fig. 8 shows the processes of convergence until 800 iterations in Fig. 6(a) of N-O-NF-OA. Please note that N-O-NF-OA is recommended in this study for the present node-based design since it eliminates the typical disadvantages of element-based design, i.e., checkerboard patterns and jagged boundaries, through a novel node-based design without using a filter method and regularization.

Fig. 9 sketches the converged curves of element and node based design under the design conditions shown in Table 1. As can be seen, the regularization method provides lower converged values of objective function in both type A and type B. In addition, type A without the use of the filter method requires more optimization steps in order to be converged like other cases.

6. Conclusions

This study had two main objectives. One was to evaluate desired optimal material reinforcement layouts of steel plates that eliminate the "checkerboard" effect and jagged boundaries that usually occur in typical element-based design for material topology optimization. The desired results may be practically applied in engineering design. In order to achieve them, a novel node-based design is presented in this study. In particular, N-O-NF-OA is recommended in this study since it only utilizes the substance of node-based design. The other objective was to understand the principles and characteristics of the present node-based design through a comparison with conventional element-based material topology optimization.

By evaluating the shape and topology results of numerical examples, it is found that the present node-based design may be an alternative to element-based design for the fields of material topology optimization. In further research, practical examples that apply the verified CCARAT optimizer will be examined.

Acknowledgements

This research was supported by the MKE (The Ministry of Knowledge Economy), Korea, under the Convergence-ITRC (Convergence Information Technology Research Center), supervised by the NIPA(National IT Industry Promotion Agency), (NIPA-2013-H0401-13-1003) and a grant (code# 2010-0019373, 2012R1A2A1A01007405, 2012-0004291 & 2013R1A1A2057502) from the National Research Foundation of Korea (NRF) funded by the Korea government. This study was financially supported by Pusan National University under the Post-Doc. 2010 program.

References

Hagishita, T. and Ohsaki, M. (2009), "Topology optimization of trusses by growing ground structure method", *Struct. Multidiscip. Opt.*, **37**(4), 377-393.

Ali, M.A. and White, R.N. (2001), "Automatic generation of truss model of optimal design of reinforced concrete structures", *ACI Struct. J.*, **98**(4), 431-442.

Biondini, F. and Bontempi, F. and Malerba, P.G. (2001), "Stress path adapting strut-and-tie models in cracked and uncracked R.C. elements", *Struct. Eng. Mech.*, **12**(6), 685-698.

Andreassen, E., Clausen, A., Schevenels, M., Lazarov, B.S. and Sigmund, O. (2011), "Efficient topology optimization in MATLAB using 88 lines of code", *Struct. Multidiscip. Opt.*, **43**(1), 1-16.

Bendsøe, M.P. and Kikuchi, N. (1988), "Generating Optimal Topologies in Optimal Design using a Homogenization Method", *Comput. Methods Appl. Mech. Eng.*, **71**, 197-224.

Amstutz, S. (2011), "Connections between topological sensitivity analysis and material interpolation scheme in topology optimization", *Struct. Multidiscip. Opt.*, **43**(6), 755-765.

Gerzen, N. and Barthold, F.J. (2012), "Enhanced analysis of design sensitivities in topology optimization", *Struct. Multidiscip. Opt.*, **46**(4), 585-595.

Haug, E.J., Choi, K.K. and Komkov, V. (1986), *Design Sensitivity Analysis of Structural Systems*, Academic Press, New York.

Ma, J., Wang, M.Y. and Zhu, X. (2011), "Compliant fixture layout design using topology optimization method", *IEEE International Conference on Robotics and Automation, ICRA 2011*, Shanghai, China.

Byun, J.K., Lee, J.H. and Park, I.H. (2004), "Node Based Distribution of Material Properties for Topology Optimization of Electromagnetic Devices", *IEEE Tran. Magnet.*, **40**(2), 1212-1215.

Sigmund, O. (2001), "A 99 topology optimization code written in Matlab", *Struct. Multidisc. Optim.*, **21**, 120-127.

Maute, K. and Ramm, E. (1995), "Adaptive topology optimization", *Struct. Optim.*, **10**, 100-112.

Gunwant, D. and Misra, A. (2012), "Topology optimization of continuum structures using optimality criterion approach in ANSYS", *Int. J. Adv. Eng. Tech.*, **5**(1), 470-485.

Patnaik, S.N., Guptill, D.J. and Berke, L. (1995), "Merits and limitations of optimality criteria method for structural optimization", *Int. J. Numer. Method. Eng.*, **38**, 3087-3120.

CARAT (2000), *Programsystem CARAT, Eingabebeschreibung und Dokumentation*, Unveroeffentlichter Bericht des Institute fuer Baustatik, Universitaet Stuttgart.

Tiyyagura, S.R. and Von Scheven, M. (2007), "FSI simulations on vector systems-development of a linear iterative solver (BLIS)", *High Perform. Comput. Vec. Syst.*, 167-177.

Chan, C.M. and Wong, K.M. (2008), "Structural topology and element sizing design optimization of tall steel frameworks using a hybrid OC-GA method", *Struct. Multidisc. Optim.*, **35**(5), 473-488.

Chan, C.M. (2005), "An optimality criteria algorithm for tall steel building design using commercial standard sections", *Struct. Multidisc. Optim.*, **5**(1-2), 26-29.

Huang, X. and Xie, Y.M. (2010), "Evolutionary topology optimization of continuum structures with an additional displacement constraint", *Struct. Eng. Mech.*, **34**(5), 581-595.

Otomiri, M., Andkjaer, J., Sigmund, O., Izui, K. and Nishiwaki, S. (2012), "Inverse design of dielectric materials by topology optimization", *Prog. Electrom. Res.*, **127**, 93-120.

Lee, D.K., Lee, J.H. and Ahn, N.S. (2014), "Generation of structural layout in use for '0-1' material considering n-order eigenfrequency dependence", *Mater. Res. Innov.*, **18**(2), 833-839.

Lee, D.K., Lee, J.H., Lee, K.H. and Ahn, N.S. (2014), "Evaluating topological optimized layout of building structures by using nodal material density based bilinear interpolation", *J. Asian Arch. Build. Eng.*, **13**(2), 421-428.